THE JOURNAL OF COMPARATIVE NEUROLOGY 398:98–104 (1998)

Merkel Complexes of Human Digital Skin: Three-Dimensional Imaging With Confocal Laser Microscopy and Double Immunofluorescence

D. GUINARD,[1]* Y. USSON,[2] C. GUILLERMET,[3] AND R. SAXOD[1]
[1]Equipe de Neurobiologie du Développement, LAPSEN-U 318, Université Joseph Fourier, BP 53-38041 Grenoble, France
[2]TIM C UMR 5525 CNRS Institut Albert Bonniot, Université Joseph Fourier, CHRU Grenoble 38043, France
[3]Laboratoire de Pathologie Cellulaire, Centre Hospitalier Universitaire de Grenoble, BP 217-38043 Grenoble, France

ABSTRACT

Three-dimensional (3-D) reconstruction of images provided by confocal scanning laser microscopy (CSLM) is a powerful tool in a morpho-functional approach to cutaneous innervation studies. To investigate mechanoreceptors in the hand, a study of Merkel complexes was performed in human finger. A double fluorescent-conjugated immunolabeling with antibodies against neurofilament (NF 200) and cytokeratin (CK 20) on floating, thick cutaneous samples (80 to 100 μm), was used. After acquisition of serial optical planes by CSLM, reconstruction was performed with 3-D reconstruction software tools. Merkel cells were clearly labeled with CK 20, whereas nerve components were only NF 200 reactive. The cells, localized on the basal lamina of the epidermis, were usually arranged in clusters of five to eight cells. Each cell was connected to a nerve process ramification originating from a unique fiber. Quantitative data, compiled from a sample of 25 Merkel complexes, gave a mean cell diameter of 13 ± 1 μm and a mean nerve fiber size of 3 ± 1 μm. Surface measurements were done on a single reconstructed cluster with a mean and standard error which only refers to the optical 3-D resolution. It gives a surface of 12 ± 1 μm^2 for the contact zone between cell and nerve fiber and a cluster area of about 500 μm^2. The great precision of reconstructed images provides a detailed analysis of spatial relationships between abutting nerve fibers and Merkel cells. Data interpretation is improved with complementary ultrastructural and physiological studies results, and this allows an accurate investigation of cutaneous sensory endings. J. Comp. Neurol. 398:98–104, 1998.

Indexing terms: mechanoreceptors; 3-D reconstruction; skin innervation

Since the first work of Crowe and Whitear in 1978, immunolabeling techniques have developed as the most reliable means for the identification of histological structures, particularly neural ones. By using these techniques, numerous neuropeptides and proteins have been reported in cutaneous sensory endings (i.e., calcitonin gene-related peptide, CGRP; chromogranin, CGA; vasoactive-intestinal-peptide, VIP; neuron specific enolase, NSE; protein-gene-product 9.5, PGP 9.5; Gu et al., 1981; Thompson et al., 1983; Björklund et al., 1986; Hartschuh et al., 1989; Wang et al., 1990; Karanth et al., 1991; Kennedy and Wendelschafer-Grabb, 1993) and thus constitute many potential and specific markers for the study of skin innervation in greater depth. Antibodies against neurofilaments (NF 70-200; Iwanaga et al., 1982; Dalsgaard et al., 1984; Björklund et al., 1986) or against PGP 9.5 (Thompson et al., 1983; Wang et al., 1990; Kennedy and Wendelschafer-Grabb, 1993; Rumio et al., 1995) have proved to be reliable specific markers of nerve fibers and/or endings. Merkel described, in 1875, large clear epidermal cells, isolated or assembled in groups, located on the basal lamina, in close contact with basal keratinocytes. As they were connected

*Correspondence to: D. Guinard, Equipe de Neurobiologie du Développement, LAPSEN-U 318, Université Joseph Fourier, BP 53-38041 Grenoble Cedex 9, France. E-mail: Didier.Guinard@ujf-grenoble.fr

Received 22 July 1997; Revised 31 March 1998; Accepted 10 April 1998

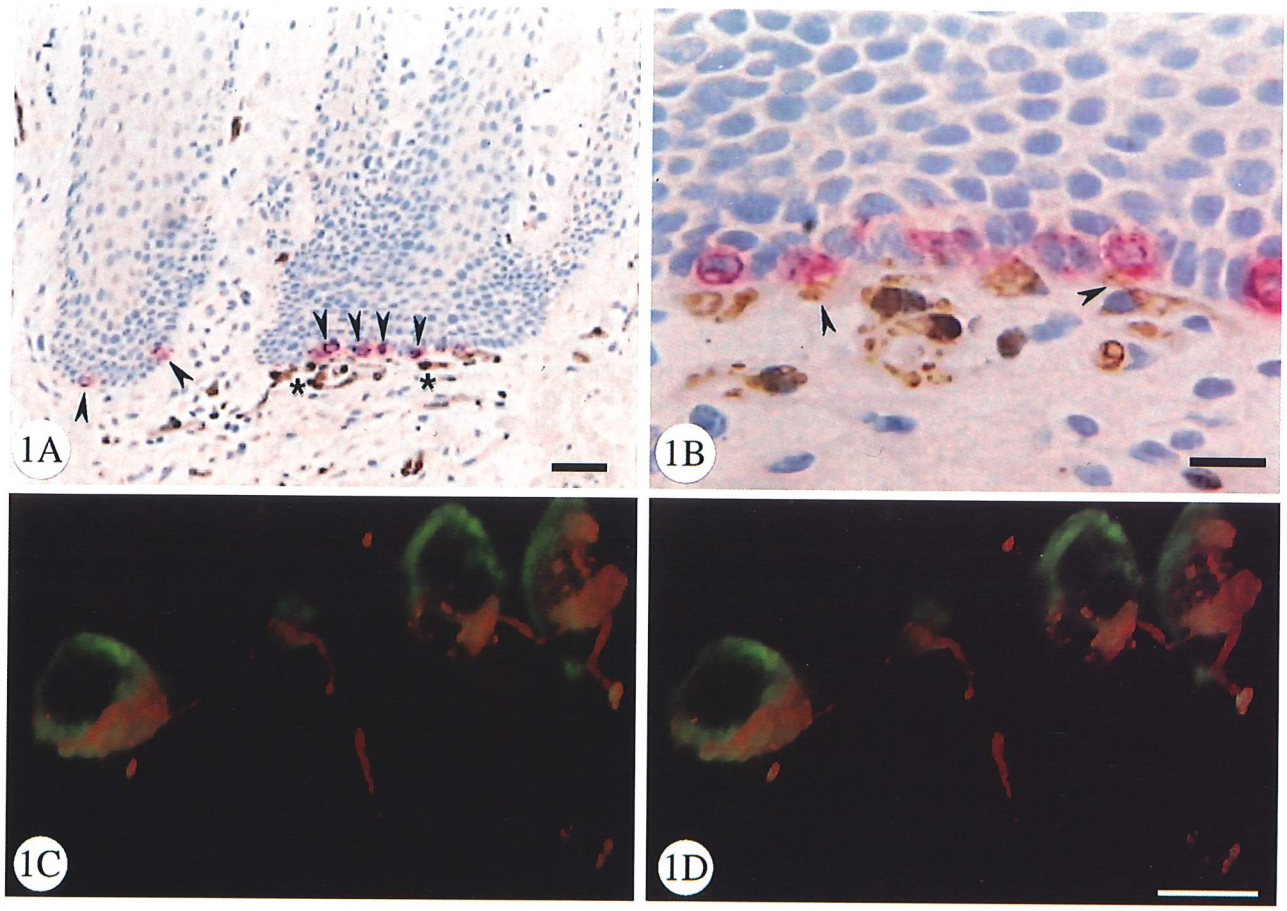

Fig. 1. **A:** General view of a digital pulp section stained with anti-cytokeratin 20 (in red) and anti-S 100 protein (in brown) antibodies. Merkel cells are present at the base of one ridge of the epidermis (arrowheads), and dermal nerve fibers, revealed by anti-S 100 protein staining of the Schwann sheath, are seen in the immediate vicinity (stars) of the epidermis. Thin paraffin sections (7 μm). Hematoxylin counterstaining. Light microscopy. 10×. **B:** High magnification of another section. Merkel cells are situated on the basal lamina of epidermis in close contact with basal keratinocytes. Labeling is strictly cytoplasmic, and nuclei are clearly visible. Dermal nerve fibers (brown) are seen making contact (arrowheads) with Merkel cells. 40×. **C,D:** Stereo-pair (cross-eyed vision) of a cluster of Merkel complexes, stained with anti-NF 200 (red) and anti-CK 20 (green) fluorescent-conjugated antibodies, obtained from 70 serial optical sections of 0.3 μm (CSLM, laser Argon 488 nm). Ray casting method reconstruction. Lens 40/1.30. Scale bars = 50 μm in A, 10 μm in B–D.

by nerves, their discoverer interpreted them as sensory endings, the Merkel–neurite complex. Until recently, they were difficult to recognize by light microscopy (LM), and extensive morphological studies with transmission electron microscopy (TEM; Breatnach, 1977; Chouchkov, 1978; Hartschuh and Weihe, 1980; Saxod, 1980, 1996; Winkelmann, 1988; Tachibana, 1995), despite their precision, brought little information about the spatial arrangement, shape, and location of Merkel cells. However, Moll et al. (1984, 1992, 1995) demonstrated that cytokeratins (CK 8-18, CK 20), which decorate the intermediate filament cytoplasmic network, are specific markers of Merkel cells in human fetal and adult skin, thus allowing easy identification at the LM level (Fig. 1A,B).

Confocal scanning laser microscopy (CSLM) has supplanted stereological methods applied to serial two-dimensional images, collected by LM or TEM, for volume reconstruction of biological objects (Castano and Ventura, 1978; Saxod, 1996).

Three-dimensional (3-D) reconstruction appears to be the most reliable and accurate way to study these structures and their relationships to their environment (Castano et al., 1993). It is now possible to study morphology and organization of structures with greater precision by using thick samples, allowing an "in toto" vision. With CSLM, images can be obtained with good contrast and high resolution. By the virtual rotation in space of a given structure, appropriate computer software allows a more accurate visualization and interpretation of anatomical structures than was previously possible. Peripheral cutaneous structures have been thus studied by Castano et al. (1995) and Rumio et al. (1995) who made 3-D reconstructions of Meissner corpuscles in human skin with PGP 9.5 immunolabeling.

For complex structures like cutaneous mechanoreceptors, the simultaneous use of different fluorescent-conjugated markers, whose specificity of labeling and spectrum allows fine identification of different components of the same structure, coupled with CSLM observation, increases the possibilities of interpretation and reconstruction (Shotton, 1989; Parazza et al., 1993). The present study uses double immunolabeling and CSLM to investigate Merkel complexes in human digital skin.

MATERIALS AND METHODS

Tissue preparation

Human digital pulps of two second digits, obtained from non-replantable traumatic amputations, provided by the Hand Surgery Unit at Grenoble University Hospital (France), were used. Injuries occurred in the dominant hand of two manual workers (43 and 51 years old) without any noticeable medical antecedents, and their informed consent was completed in accordance with Helsinki regulations. Samples were immediately excised and fixed in 4% formaldehyde-phosphate-buffered saline (PBS) 0.01 M, pH 7.4, for 24 hours at 4°C. After rinsing in distilled water, pulp tissue was cut under the microscope into small fragments, perpendicular to the skin surface (1 × 6 × 3 mm), and immediately embedded in paraffin or in agar. Thick serial sections (80 to 100 µm) were made from both paraffin- and agar-embedded samples with a vibratome (Vibraslice 752 M, Campden Instruments LTD, England) and treated for immunolabeling.

Immunofluorescence and immunochemistry

Two equivalent series of paraffin- and agar-embedded samples were done in parallel by using a floating technique and double-immunofluorescence labeling. After being deparaffinized with toluene and rehydrated in graded concentrations of ethanol when necessary, all samples were treated by microwaves (Micromat 120 AEG, Frequency 2.45 Hz, 850 W) in sodium citrate buffer 0.01 M, pH 6, for 2 cycles of 5 minutes each, in order to facilitate labeling. After incubation in 0.01 M PBS, pH 7.4, containing 2% skimmed milk powder, in a humid atmosphere at 4°C for 1 hour and rinsing, sections were floated in a mixture of two primary antibodies, applied for 48 hours at 4°C: murine monoclonal antibodies to cytokeratin 20 (CK 20; Biogenex, San Ramon, CA) at a dilution of 1:200 and rabbit polyclonal antibodies to neurofilament (NF 200; Sigma, St. Louis, MO) at a dilution of 1:250, in a humid atmosphere with gentle agitation. After rinses in 0.01 M PBS, pH 8.6 (3 × 20 minutes) and incubation in 1% bovine serum albumin (BSA) for 30 minutes, secondary fluorescent-conjugated antibodies were sequentially applied at 4°C, in a humid and dark atmosphere, for 3 hours. A 0.01 M PBS, pH 8.6, rinse (1 hour) followed by 1% BSA (30 minutes), between the two sequences, was done. The sections were first incubated in rhodamine-conjugated (TRITC) goat anti-rabbit antibodies (Jackson, West Grove, PA) at 1:100, for NF 200 labeling, and further by fluorescein-conjugated (FITC) rabbit-antimurine antibodies (Dako, Glostrup, Denmark) at 1:75, for identification of CK 20. After a final rinse in 0.01 M PBS, pH 8.6, for 1 hour, sections were mounted in an antifading medium (TRIS-HCL, pH 7.6, 0.05 M [10%], glycerol [90%], 1.4 diazabicyclo-octan 2% [Sigma D 2522]) between a slide and a coverslip sealed by nail varnish.

For control sections, primary antibodies were substituted by nonimmune murine and rabbit IgG (2 mg/ml) (Jackson), or by eliminating the first incubation.

For conventional light microscopy, 7-µm sections were obtained from paraffin, embedded samples and immunochemistry was performed, as described above, with monoclonal antibodies to cytokeratin 20 (Biogenex, San Ramon, CA) and rabbit polyclonal antibodies to S 100 protein (Immunotech 1071, Marseille, France). Specific staining was revealed by incubation with biotinylated secondary antibodies followed either by a peroxidase (for S 100 protein) or fast red phosphatase (for CK 20) conjugated avidin-biotin complex (1:500, 1 hour). Peroxidase was revealed by using di-amino-benzidine tetrahydrochloride, and nuclei were counterstained with hematoxylin.

Confocal microscopy

Confocal optical sections were collected with a confocal scanning laser microscope, LSM 410 Invert (Carl Zeiss, Freiburg), by using a 40× objective lens (Plan-Neofluoar, 1.3 NA, oil immersion). Simultaneous imaging of FITC and TRITC fluorescence was performed with the following settings: Both labels were excited with the 488-nm line of an Argon laser; a 510-nm dichroic mirror was used to separate the excitation beam from the emitted fluorescence. The radiation from each fluorochrome was segregated by means of a 560-nm beam splitter, and label emissions were selected with a 520- to 560-nm band-pass filter (FITC) and a 590-nm long-pass filter (TRITC).

Two different samplings were used: The high-resolution imaging of a single Merkel cell (Fig. 3A–C) was obtained by

Fig. 2. **A:** 3-D reconstruction by a ray casting method of a cluster of Merkel complexes labeled by fluorescent-conjugated antibodies against NF 200 (red) and CK-20 (green) obtained from 134 serial optical sections of 0.3 µm (CSLM, laser Argon 488 nm). Several Merkel cells, arranged in a semicircular row at the extremity of an epidermal crest, are connected by a nerve afferent fiber. Cluster area (80 ± 1 × 100 ± 1 µm) measures about 500 µm², and mean cell diameter is 15 ± 1 µm. Epidermis on top. Arrow indicates the cell reconstructed in Figure 3A–C. Measurement mean and standard error only refers to 3-D optical resolution. Reconstructed final volume of 77 × 77 × 40 µm. Lens 40/1.30. **B:** 3-D reconstruction by a surface shading method of the same cluster as in A. The globulous shape of Merkel cells is clearly visible. Merkel cells are connected by a unique nerve fiber (star) which divides into ramifications, with a termination of nerve branches in flat endings. **C:** 3-D reconstruction of the same cluster as in A with a rotation of 90° along the X axis with respect to A. The cluster is seen from above, as it would be observed "through" the epidermis. The afferent nerve fiber (star) and its ramifications are clearly identified. **D:** 3-D reconstruction of the same cluster as in A with a rotation of 90° along the Y axis with respect to A. Limits of the section are clearly visible on the left and right of the image. The cell assembly is on the same plane, on the basal lamina of the epidermis. The afferent nerve trunk (star) has several branches, and the zone of contact, between the nerve and the cell, is located on the basal side of the cell. Scale bar = 10 µm.

Fig. 3. **A:** 3-D reconstruction by a ray casting method of a Merkel cell (cell indicated by an arrow in Figure 2A) labeled by fluorescent-conjugated antibodies against NF 200 (red) and CK-20 (green) obtained from 46 serial optical sections of 0.3 µm (CSLM, laser Argon 488 nm). The afferent nerve fiber (diameter 2.5 ± 1 µm) presents a torsion along its longitudinal axis and a curve of 180° before reaching the cell. The heterogeneous center part is clearly devoid of CK 20 labeling probably in relation to the presence of the nucleus. Measurement mean and standard error only refers to 3-D optical resolution. Reconstructed final volume of 19 × 19 × 14 µm. Lens 40/1.30. **B:** 3-D reconstruction by a surface shading method of a Merkel cell (cell of A). The globulous shape of the cell is clearly visible. Before reaching the cell, the afferent fiber describes curves with a thin preterminal portion (arrow) which can be interpreted as the basal lamina crossing region. The zone of contact is enlarged and flattened with an area of 12 ± 1 µm². Cytoplasmic labeling is high at the periphery, then more heterogeneous or absent in the center, where the nucleus is. **C:** Same 3-D reconstruction of a Merkel cell as in B with a rotation of 75° around the Y axis. The intimate relationship between the base of the cell and the flattened nerve terminal is clearly visible. The surface of contact between the cell and the nerve plate represents about one-third of the entire cell surface. Scale bar = 5 µm.

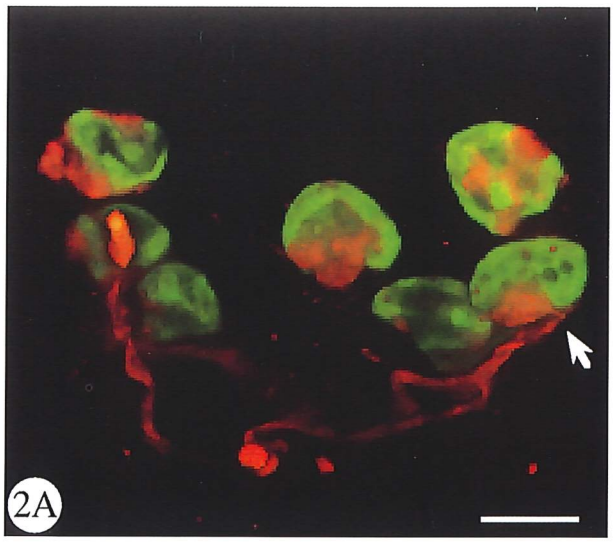

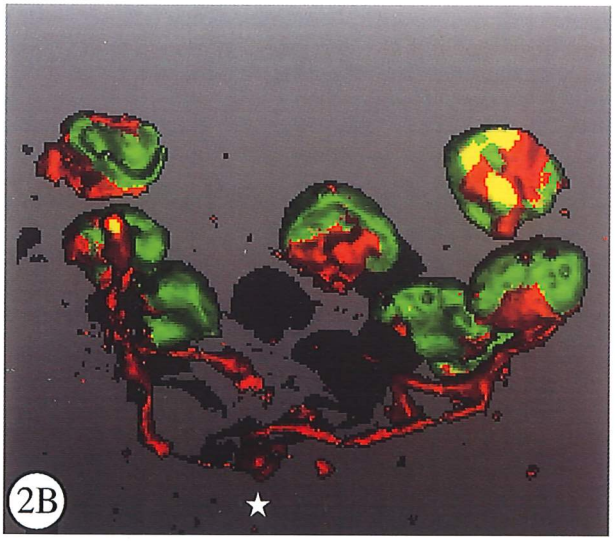

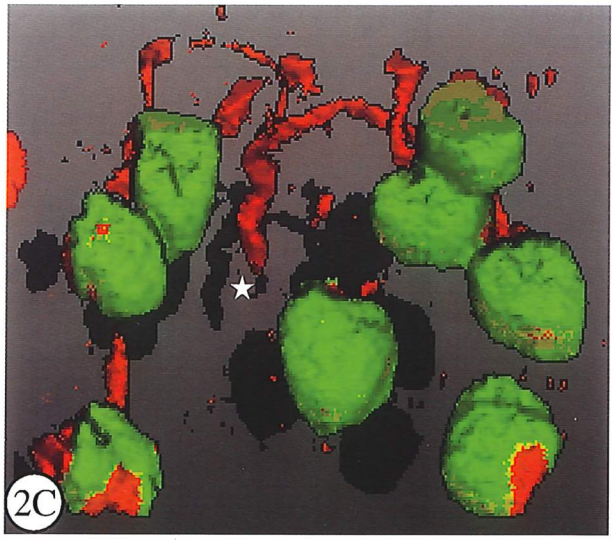

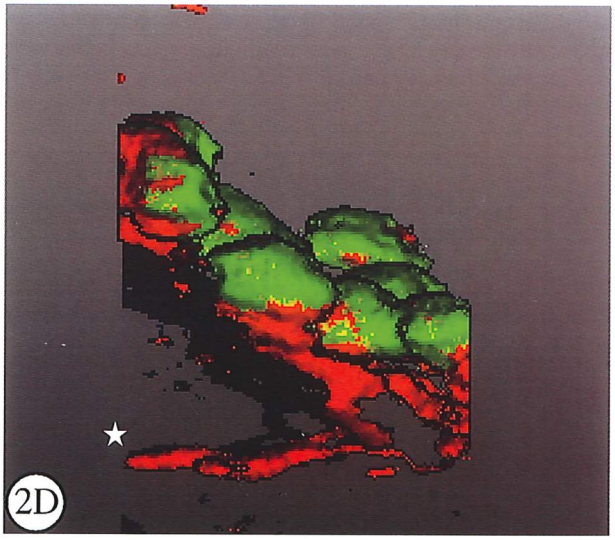

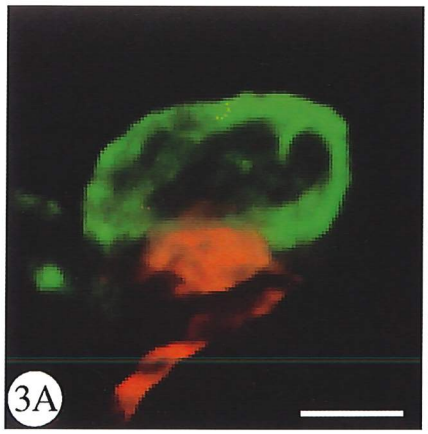

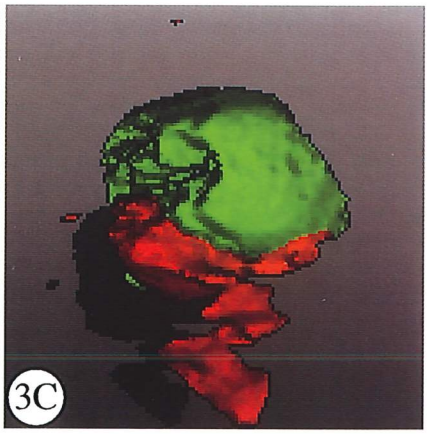

Figures 2 and 3

collecting 46 serial optical sections every 0.3 μm with a pixel size of 0.15 μm; the imaging of the clusters of Merkel cells was obtained by collecting 70 (Fig. 1C,D) and 134 (Fig. 2A–D) optical sections every 0.3 μm with a pixel size of 0.3 μm. Each optical section was obtained by averaging eight frames in order to improve the signal-to-noise ratio. During the tomography session, a correction of attenuation of emitted and reflected light, due to sample penetration, was necessary by means of a gain compensation of the photomultiplier (voltage magnification). Neither TRITC nor FITC fluorescence presented problems of bleaching during sessions, even for long exposures (more than 10 minutes/50 optical sections).

Three-dimensional reconstruction

The stacks of images were edited and reconstructed with software developed in our laboratory (Parraza et al., 1993) and running on Silicon Graphics workstations and on Power Macintosh computers. Briefly, the stack of optical sections was processed in order to compensate for the decay of fluorescence intensity as a function of depth in the tissue. The signal-to-noise ratio was improved by applying a 3-D median filter to the data set. The volumes were visualized with two different rendering approaches: surface shading and ray casting. These visualization tools are based on 3-D reconstruction techniques in which the basic principle is to create either a still or animated synthetic image of the volume. Different visual attributes can be selected in order to render specific information. The two main attributes are 1) the shape of the observed objects (cells, nuclei . . .), which implies a surface rendering approach (surface shading), and 2) the content of the object, which implies a transparency rendering of volumes (ray casting). By contrast, in the surface model, only the surface voxels are considered; that is achieved when showing solid objects as the volume model claims to show all the information contained in the 3-D cube. This last display mode might be called "see-through" or transparent viewing.

RESULTS

On thin paraffin sections examined by conventional light microscopy, Merkel cells appeared to be specifically labeled by anti-CK 20 antibodies (Fig. 1A,B) and were present at the base of certain ridges of the epidermis. After labeling with anti-S 100 protein, to reveal the Schwann sheath of nerve fibers, nerve terminals can be seen making contacts (Fig. 1B, arrowheads) with Merkel cells. For CSLM, agar embedding proved to be better than paraffin for immunofluorescent labeling of thick sections, perhaps because paraffin embedding may alter thick samples and interfere with antibody penetration. CSLM observation is visually demanding, and plotting of fluorescent objects in thick samples can be difficult. Furthermore, the observed structure must be completely scanned in order to achieve a satisfactory reconstruction. Several clusters were examined; three were analyzed in detail (Figs. 1C,D, 2A–D), but only one was totally reconstructed as well as one Merkel cell with its nerve terminal at a higher magnification (Fig. 3A–C). In order to enhance qualitative data, 3-D reconstruction was performed by a surface rendering approach or a ray casting method according to the structures studied (shape of the object [cells, nuclei . . .], content of the object). Labeling was specific for each component (CK 20 for the cell, NF 200 for the nerve), and there was no fluorescence blurring which might have interfered with interpretation. Merkel complexes appeared in groups (clusters) of cells at the extremity of an epidermal ridge, usually in a semicircular arrangement (Figs. 1C,D, 2A–C). Merkel cells, clearly labeled by antibodies against CK 20, were globular in shape, with a flat base, and situated along the same plane. Measurements, taken on a selection of 25 cells from three observed clusters (not shown), gave a mean cell diameter of 13 ± 1 μm (range: 7.5–17 μm). Each cell was connected by a thin nerve ramification, marked for NF 200, originating from a unique afferent fiber. In some instances, the same ramification seemed to connect two neighboring cells (Fig. 2D). The mean size of nerve fibers, of the three clusters analyzed (not shown), was 3 ± 1 μm (range 2–4 μm, mean measurements on 25 fibers).

In Merkel cells, the green fluorescence, caused by anti-CK 210 antibodies, was diffuse and heterogeneous, dense at the periphery but absent in the center. This lack of labeling could be interpreted as the location of the nucleus, as labeling by antibodies against CK 20 was strictly limited to keratin network fibers which are only cytoplasmic (Fig. 3A,B). The flat basal surface entered into contact with the nerve ending, a region that we interpret as the transduction zone (Fig. 3B,C). The nerve fiber followed a spiral course before reaching the cell and presented a discoïdal adherent nerve plate which seemed to support the dermal side of the cell (Fig. 3C). Surface and size measurements, done on a single reconstructed cluster (Fig. 2A–D) and reconstructed cell (Fig. 3A–C) have a mean and standard error which only refers to the optical 3-D resolution. The elliptic plane of the reconstructed cluster was about 80 ± 1 μm in width and 100 ± 1 μm in length, and its area was about 500 μm^2 (Fig. 2A). The nerve plate surface, which occupied about one-third of the cell base, was 12 ± 1 μm^2 (Fig. 3A–C).

DISCUSSION

In 1875, using an osmic acid preparation, Merkel described a large clear epidermic cell connected by nerves which he interpreted as a sensory ending. Although its ectodermic or neural crest origin has not been definitively proved in humans yet (Moll and Moll, 1992; Tachibana, 1995; Saxod, 1996), several neural and epidermal markers have been demonstrated, allowing specific identification at the light microscopic (LM) level. The Merkel cell is reactive for several neuropeptides and proteins such as neuron specific enolase (NSE), protein gene product 9.5 (PGP 9.5), chromogranin (CGA), vasoactive intestinal polypeptide (VIP), calcium gene–related polypeptide (CGRP), and metenkephalin in animal species and humans (Gu et al., 1981; Hartschuh et al., 1989; Karanth et al., 1991; Tachibana, 1995). Moll et al. (1984, 1995) have demonstrated that cytokeratins 8–18 and 20 (CK 8–18, CK 20) are specific and reliable labels for Merkel cells in human adult and fetal skin.

The contact between a nerve fiber and a Merkel cell with immunolabeling techniques at the LM level has rarely been demonstrated. Moll et al. (1984) reported such a case after double immunolabeling with antibodies against cytokeratins (CK 8–18) and neurofilaments (NF 70–200). However, Narisawa et al. (1994) have shown that, in certain preneoplasic status, about 10% of the Merkel cells react with NF 70–200, which may interfere with image interpretation when this antibody is used for simultaneous immunolabeling. Gu et al. (1981), using antibodies against

NSE, demonstrated nerve fibers close to Merkel cells but no convincing connections. With PGP 9.5, Wang et al. (1990) also demonstrated close relations between nerve ramifications and Merkel cells. Rumio et al. (1995), with CSLM and PGP 9.5 immunolabeling, reported confocal images of Merkel cells but without evidence of a contact region between the cell and the nerve ending, probably due to a lack of labeling. Almost all Merkel cells are innervated (Pasche et al., 1990), and in the present study, noninnervated cells were never observed. From our knowledge, this is the first time that a convincing connection has been demonstrated between a Merkel cell and an afferent nerve with an immunolabeling technique and CSLM.

The principal advantage of double labeling is an objective visualization and image interpretation of structures. In our reconstructions, Merkel cells are only CK 20 reactive, the nervous structure being strictly labeled by NF 200, and no fluorescence blurring troubles interpretation. The neural connection has, however, been reported by several TEM studies in animals and humans, describing a contact region on the basal side of the cell and dense intracytoplasmic core granules (70 to 120 nm) localized at the dermal side of the cell, next to the nerve terminal (Breatnach, 1977; Saxod, 1978; Hartschuh and Weihe, 1980; Winkelmann, 1988). According to Tachibana (1995), the Merkel cell population in human skin can be divided into two groups: innervated and noninnervated cells. The former type might act, during skin development and post-traumatic reinnervation, as targets for nerve guiding and sprouting by means of the release of trophic factors. In the course of skin differentiation, a reciprocal trophic dependence between nerves and Merkel cells has been demonstrated (Pasche et al., 1990; Vos et al., 1991; Narisawa et al., 1992, 1996; Moll et al., 1996). Merkel cells could play a role of metabolic support for intra-epidermal nerve terminals as well as for capillaries and conjunctive cells. Noninnervated Merkel cells in adult skin can also stimulate differentiation of keratinocytes and modulate sensory nerve endings (Gaudillère and Misery, 1994).

This close relationship between the basal membrane of the Merkel cell and nerve endings, the presence of specialized junctions, and rare observations of fusion between core granules and cell membrane (Chen et al., 1973) are in favor of a chemical synaptic transmission. Merkel cells act as mechanical transducers (Horch et al., 1974; Iggo and Findlater, 1984; English et al., 1992), this functional aspect being supported by experiments with Ca^{2+} channel blockers (Findlater et al., 1987; Pacitti and Findlater, 1988). However, this question is still controversial (Mills and Diamond, 1995), and the possibility of a prime mechanical transduction by the nerve ending remains (Gottschaldt and Vahle-Hinz, 1981; Diamond et al., 1988; Diamond, 1994; Gaudillère and Misery, 1994).

The arrangement of Merkel cells in clusters, connected by a single nerve fiber, can argue for a collective physiological behavior, but this may be discordant with electrophysiological data. Evaluation of cutaneous Merkel cell densities, extrapolated from microneurographic recordings of human digital nerves, is a hundred times lower than those obtained by histological methods (Miller et al., 1958; Johansson and Vallbö, 1979; Vallbö and Johansson, 1984; Lacour et al., 1991; McKenna Boot et al., 1992; Cohen and Vierck, 1993; Thomas and Westling, 1995). Nevertheless, according to the strategy of histological counting, results can vary greatly. Furthermore, noninnervated cells (anatomically and/or physiologically speaking) would be counted with a histological approach, whereas they would not be detected by electrophysiology. These differences can also be explained by the fact that Merkel cells, assembled in clusters and connected by a single nerve, can act not as a single physiological unit as the spatial orientation could suggest, but perhaps more as autonomic entities. Merkel cells are considered type I slowly adapting mechanoreceptors (SA I) (Horch et al., 1974), and the evaluation of SA I unit densities can be very different depending on whether the cell physiological behavior is individual or collective. Type I mechanoreceptor (SA I and RA I) recordings for edge sensitivity in digital pulp sensitive fields (Johansson et al., 1982) are in favor of a possible peripheral coding of information. The SA I units have a better edge sensitivity than RA I receptors, so signal modulation may perhaps be produced in the skin in relation to the spatial arrangement of Merkel cells among a given cluster and/or between several clusters which may have been stimulated, owing to the possibility of the transmission of a slight skin deformation at distance. The surface occupied by a cluster reaches about 500 μm^2, according to our observation, but electrophysiological evaluation when assessed by standardized methods (Vallbö and Johansson, 1984) give surfaces of 11 mm^2 for such SA I receptive fields with distinct borders. Thus, responses from a unique SA I receptive field (SA I unit) seem to reflect the activation of several clusters of Merkel cells which would mean that there is already a structured (integrated) coding at the periphery level. These discrepancies of interpretation between histological and physiological data plead for a collective physiological behavior of Merkel cells. However, explanation of the physiology requires further experimental studies.

Usually Merkel complexes are situated with a horizontal orientation, on the basal lamina of epidermis, in close relation to basal keratinocytes, in groups of five to eight cells (cluster) at the extremity of epidermal ridges (Moll et al., 1984; Winkelmann, 1988; Tachibana, 1995). Confocal images are consistent with these descriptions. Merkel complexes are arranged in a ring or in an elliptical assembly in the same plane and are connected by small nerve ramifications originating from an unique afferent fiber. The cell has a globulous shape, and cytoplasmic labeling is heavy at the periphery and more heterogeneous in the center. As with thin immunolabeled samples, the polylobed nucleus can be easily observed on 3-D reconstructions. However, ultrastructural studies have shown that the cells have fine cytoplasmic projections which penetrate between keratinocytes. Despite high cytoplasmic labeling and the possibility of rotation, resolution is insufficient to observe these processes (Breatnach, 1977; Chouchkov, 1978; Saxod, 1978; Winkelmann, 1988; Tachibana, 1995), and only gross diverticles were seen on confocal images.

In conclusion, the use of CSLM combined with double immunofluorescence on thick sections gives detailed 3-D reconstructions of Merkel complexes and allows a clear demonstration, at the optical level, of the nerve terminal abutting the Merkel cell. These methods are powerful tools for studying the organization and relationships of mechanoreceptors and nerves involved in cutaneous innervation.

ACKNOWLEDGMENTS

We thank Pr. F. Moutet (Hand Surgery Unit, Grenoble University Hospital, France) who provided the human material, Dr. F. Labat-Moleur for valuable technical advice, Dr. L. Pays for digitized images, and Dr. F. Hemming for revising the English language of the manuscript.

LITERATURE CITED

Björklund, H., C.J. Dalsgaard, C.E. Jonsson, and A. Hermasson (1986) Sensory and autonomic innervation of non-hairy and hairy human skin. An immunohistochemical study. Cell Tissue Res. *243:*51–57.

Breatnach, A.S. (1977) Electron microscopy of cutaneous nerves and receptors. J. Invest. Dermatol. *69:*8–26.

Castano, P. and R.G. Ventura (1978) The Meissner's corpuscle of the Green-Monkey. (*Cercopithecus aetiopis L.*) J. Submicrosc. Cytol. *10:*327–344.

Castano, P., A. Marcucci, A. Miani, Jr., M. Morini, S. Veraldi, and C. Rumio (1993) Central and peripheral nervous structures as seen at the confocal scanning laser microscope. J. Microsc. *175:*229–237.

Castano, P., C. Rumio, M. Morini, A. Miani, Jr., and S.M. Castano (1995) Three-dimensional reconstruction of the Meissner's corpuscle of man after silver impregnation and immunofluorescence with PGP 9.5 antibodies using confocal scanning laser microscopy. J. Anat. *186:*261–270.

Chen, S.Y., S. Gerson, and J. Meyer (1973) The fusion of Merkel cell granules with a synapse-like structure. J. Invest. Dermatol. *61:*290–292.

Chouchkov, C. (1978) Cutaneous receptors: Ultrastructure and morphological classification. In A. Brodal, W. Hild, J. Van Limborgh, R. Ortmann, T.H. Schiebler, G. Töndury, and E. Wolff (eds): Advances in Anatomy, Embryology and Cell Biology, Vol. 54, Fasc. 5. Berlin: Springer-Verlag, pp. 9–32.

Cohen, R.H. and C.J. Vierck, Jr. (1993) Relationships between touch sensations and estimated population responses of peripheral afferent mechanoreceptors. Exp. Brain Res. *94:*120–130.

Dalsgaard, C.J., H. Björklund, C.E. Jonsson, A. Hermasson, and D. Dahl (1984) Distribution of neurofilament-immunoreactive fibers in human skin. Histochem. *81:*111–114.

Diamond, J. (1994) Nerve-skin interactions in adult and aged animals. Progr. Clin. Biol. Res. *390:*21–44.

Diamond, J., L.R. Mills, and K.M. Mearow (1988) Evidence that the Merkel cell is not the transducer in the mechanosensory Merkel cell-neurite complex. Prog. Brain Res. *74:*51–56.

English, K.B., Z.Z Wang, N. Stayner, L.J. Stensaas, H. Martin, and R.P. Tuckett (1992) Serotonin-like immunoreactivity in Merkel cells and their afferent neurons in touch domes from the hairy skin of rats. Anat. Rec. *232:*112–120.

Findlater, G.S., E.J. Cooksey, A. Anand, A.S. Paintal, and A. Iggo (1987) The effects of hypoxia on slowly adapting type I (SA I) cutaneous mechanoreceptors in the cat and rat. Somatosens. Res. *5:*1–17.

Gaudillère, A. and L. Misery (1994) La cellule de Merkel. Ann. Dermatol. Venereol. *121:*909–917.

Gottschtaldt, K.M. and C. Vahle-Hinz (1981) Merkel cell receptors: structure and transducer function. Science *214:*183–186.

Gu, J., J.M. Polak, F.J. Tapia, P.J. Marangos, and A.G.E. Pearse (1981) Neuron-specific enolase in the Merkel cells of mammalian skin. The use of specific antibody as a simple and reliable histologic marker. Am. J. Pathol. *104:*63–68.

Hartschuh, W. and E. Weihe (1980) Fine structural analysis of the synaptic junction of Merkel cell-axon-complexes. J. Invest. Dermatol. *75:*159–165.

Hartschuh, W., E. Weihe, and N. Yanaihara (1989) Immunohistochemical analysis of chromogranin A and multiple peptides in the mammalian Merkel cell: further evidence for its paraneuronal function. Arch. Histol. Cytol. *52:*423–431.

Horch, K.W., D. Whitehorn, and P.R. Burgess (1974) Impulse generation in type I cutaneous mechanoreceptors. J. Neurophysiol. *37:*267–281.

Iggo, A. and G.S. Findlater (1984) A review of Merkel cell mechanisms. In W. Hamann and A. Iggo (eds): Sensory Receptor Mechanisms. Singapore: World Scientific Publications, pp. 117–131.

Iwanaga, T., T. Fujita, Y. Takahashi, and T. Nakajima (1982) Meissner's and Pacinian corpuscles as studied by immunohistochemistry for S-100 protein, neuron-specific enolase and neurofilament protein. Neurosci. Lett. *1:*117–121.

Johansson, R.S. and A.B. Vallbö (1979) Tactile sensibility in the human hand: relative and absolute densities of four types of mechanoreceptive units in glabrous skin. J. Physiol. (Lond.) *286:*283–300.

Johansson, R.S., U. Landström, and R. Landström (1982) Sensitivity to edges of mechanoreceptive afferent units innervating the glabrous skin of the human hand. Brain Res. *244:*27–32.

Karanth, S.S., D.R. Springall, D.M. Kuhn, M.M. Levene, and J.M. Polak (1991) An immunohistochemical study of cutaneous innervation and the distribution of neuropeptides and protein gene product 9.5 in man and commonly employed laboratory animals. Am. J. Anat. *191:*369–383.

Kennedy, W.R. and G. Wendelschaber-Crabb (1993) The innervation of human epidermis. J. Neurol. Sci. *115:*184–190.

Lacour, J.P., D. Dubois, A. Pisani, and J.P. Ortonne (1991) Anatomical mapping of Merkel cells in normal adult epidermis. Br. J. Dermatol. *125:*535–542.

McKenna Boot, P., G. Rowden, and N. Walsh (1992) The distribution of Merkel cells in human fetal and adult skin. Am. J. Dermatopathol. *14:*391–396.

Miller, M.R., H.J. Ralston, and M. Kasahara (1958) The pattern of cutaneous innervation in the human hand. Am. J. Anat. *102:*183–201.

Mills, L.R. and J. Diamond (1995) Merkel cells are not the mechanosensory transducers in the touch dome of the rat. J. Neurocytol. *24:*117–134.

Moll, I. and R. Moll (1992) Early development of human Merkel cells. Exp. Dermatol. *1:*180–184.

Moll, R., I. Moll, and W.W. Franke (1984) Identification of Merkel cells in human skin by specific cytokeratin antibodies: changes of cell density and distribution in fetal and adult plantar epidermis. Differentiation *28:*136–154.

Moll, I., C. Kuhn, and R. Moll (1995) Cytokeratin 20 is a general marker of Merkel cutaneous cells while certain neuronal proteins are absent. J. Invest. Dermatol. *104:*910–915.

Moll, I., R. Paus, and R. Moll (1996) Merkel cells in mouse skin: intermediate filament pattern, localization, and hair cycle-dependent density. J. Invest. Dermatol. *106:*281–286.

Narisawa, Y., K. Haschimoto, Y. Nihei, and T. Pietruk (1992) Biological significance of dermal Merkel cells in development of cutaneous nerves in human fetal skin. J. Histochem. Cytochem. *40:*65–71.

Narisawa, Y., K. Haschimoto, and H. Kohda (1994) Immunohistochemical demonstration of the expression of neurofilaments proteins in Merkel cells. Acta Dermatol. Venereol. *74:*441–443.

Narisawa, Y., K. Haschimoto, and H. Kohda (1996) Merkel cells participate in the induction and alignment of epidermal ends of arrector pili muscles of human fetal skin. Br. J. Dermatol. *134:*494–498.

Pacitti, E.G. and G.S. Findlater (1988) Calcium channel blockers and Merkel cells. Prog. Brain Res. *74:*37–42.

Parazza, F., C. Humbert, and Y. Usson (1993) Method for 3D volumetric analysis of intranuclear fluorescence distribution in confocal microscopy. Comp. Med. Im. Graph. *17:*189–200.

Pasche, F., Y. Mérot, P. Carraux, and J.H. Saurat (1990) Relationship between Merkel cells and nerve endings during embryogenesis in the mouse epidermis. J. Invest. Dermatol. *95:*247–251.

Rumio, C., P. Castano, S. Veraldi, M. Morini, and M. Castano (1995) The innervation of human skin studied with confocal scanning laser microscopy: a comparison between PGP 9.5 immunofluorescence and silver impregnation. Neuroimage *2:*102–111.

Saxod, R. (1978) Ultrastructure of Merkel corpuscles and so-called "transitional cells" in the white leghorn chicken. Am. J. Anat. *151:*453–474.

Saxod, R. (1996) Ontogeny of the cutaneous sensory organs. Microsc. Res. Tech. *34:*313–333.

Tachibana, T. (1995) The Merkel cell: recent findings and unresolved problems. Arch. Histol. Cytol. *58:*379–396.

Thomas, C.K. and G. Westling (1995) Tactile unit properties after human spinal cervical cord injury. Brain *118:*1547–1556.

Thompson, R.J., J.F Doran, P. Jackson, A.P. Dhillon, and J. Rode (1983) PGP 9.5—a new marker for vertebrate neurons and neuroendocrine cells. Brain Res. *278:*224–228.

Shotton, M.D. (1989) Confocal scanning optical microscopy and its applications for biological specimens. J. Cell Sci. *94:*175–206.

Vallbö, A.B. and R.S. Johansson (1984) Properties of cutaneous mechanoreceptors in the human hand related to touch sensation. Hum. Neurobiol. *3:*3–14.

Vos P., F. Stark, and R.N. Pittman (1991) Merkel cells in vitro: production of nerve growth factor and selective interactions with sensory neurons. Dev. Biol. *144:*281–300.

Wang, L., M. Hilliges, T. Jernberg, D. Wiegleb-Edström, and O. Johansson (1990) Protein gene product 9.5-immunoreactive nerve fibers and cells in human skin. Cell Tissue Res. *261:*25–33.

Winkelmann, R.K. (1988) Cutaneous sensory nerves. Semin. Dermatol. *7:*236–268.